

# Krylov Linear Solvers and Quasi Monte Carlo Methods for Transport Simulations

Sam Pasmann,<sup>a</sup> C. T. Kelley,<sup>b</sup> and Ryan McClarren<sup>\*,a</sup>

*<sup>a</sup>Department of Aerospace and Mechanical Engineering  
University of Notre Dame  
Fitzpatrick Hall, Notre Dame, IN 46556*

*<sup>b</sup>North Carolina State University, Department of Mathematics  
3234 SAS Hall, Box 8205  
Raleigh NC 27695-8205*

\*Email: [rmcclarr@nd.edu](mailto:rmcclarr@nd.edu)

Number of pages: 13

Number of tables: 4

Number of figures: 5

## **Abstract**

QMC + Krylov

**Keywords** — Quasi Monte Carlo Methods, Krylov Linear Solvers

## I. INTRODUCTION

## II. COMPUTATIONAL RESULTS

In this section we consider an example from [1]. The formulation of the transport problem is taken from [2]. The equation for the angular flux  $\psi$  is

$$\mu \frac{\partial \psi}{\partial x}(x, \mu) + \Sigma_t(x) \psi(x, \mu) = \frac{1}{2} \left[ \Sigma_s(x) \int_{-1}^1 \psi(x, \mu') d\mu' + q(x) \right] \text{ for } 0 \leq x \leq \tau \quad (1)$$

The boundary conditions are

$$\psi(0, \mu) = \psi_l(\mu), \mu > 0; \psi(\tau, \mu) = \psi_r(\mu), \mu < 0.$$

### II.A. Multigroup Equations

In general geometry the multigroup equations are

$$\mu \frac{\partial \psi_g}{\partial x}(x, \mu) + \Sigma_{t,g}(x) \psi_g(x, \mu) = \frac{1}{2} \sum_{g'=1}^G \Sigma_{s,g' \rightarrow g}(x) \int_{-1}^1 \psi_{g'}(x, \mu') d\mu' + \frac{q_g(x)}{2} \quad g = 1, \dots, G. \quad (2)$$

The boundary conditions are

$$\psi_g(0, \mu) = \psi_{l,g}(\mu), \mu > 0; \psi_g(\tau, \mu) = \psi_{r,g}(\mu), \mu < 0.$$

In matrix form, these equations are

$$\mu \frac{\partial \vec{\psi}}{\partial x}(x, \mu) + \underline{\Sigma}_t(x) \vec{\psi}(x, \mu) = \frac{1}{2} \underline{\Sigma}_s(x) \int_{-1}^1 \vec{\psi}(x, \mu') d\mu' + \frac{\vec{q}(x)}{2}, \quad (3)$$

where

$$\vec{\psi} = (\psi_1, \psi_2, \dots, \psi_G)^T, \quad \vec{q} = (q_1, q_2, \dots, q_G)^T, \quad (4)$$

$$\underline{\Sigma}_t(x) = \begin{pmatrix} \Sigma_{t,1}(x) & 0 & \dots \\ 0 & \Sigma_{t,2}(x) & 0 \dots \\ \vdots & & \ddots \\ 0 & \dots & 0 & \Sigma_{t,G}(x) \end{pmatrix}, \quad (5)$$

and

$$\underline{\Sigma}_s(x) = \begin{pmatrix} \Sigma_{s,1 \rightarrow 1}(x) & \Sigma_{s,2 \rightarrow 1}(x) & \dots & \Sigma_{s,G \rightarrow 1}(x) \\ \Sigma_{s,2 \rightarrow 1}(x) & \Sigma_{s,2 \rightarrow 1}(x) & \dots & \Sigma_{s,G \rightarrow 2}(x) \\ \vdots & \vdots & & \vdots \\ \Sigma_{s,G \rightarrow 1}(x) & \Sigma_{s,G \rightarrow 1}(x) & \dots & \Sigma_{s,G \rightarrow G}(x) \end{pmatrix}, \quad (6)$$

## II.B. Source Iteration and Linear Solvers

Source iteration is Picard iteration for the fixed point problem

$$\phi = \mathcal{S}(\phi, q, \psi_l, \psi_r)$$

To use other solvers we must convert to a linear system via

$$\mathcal{K}(\phi) = \mathcal{S}(\phi, 0, 0, 0) \text{ and } f = \mathcal{S}(0, q, \psi_l, \psi_r)$$

to get

$$A\phi \equiv (I - \mathcal{K})\phi = f,$$

which we can send to a linear solver.

In the computations we use the problem from [1]

$$\tau = 5, \Sigma_s(x) = \omega_0 e^{-x/s}, \Sigma_t(x) = 1, q(x) = 0, \psi_l(\mu) = 1, \psi_r(\mu) = 0,$$

and consider two cases  $s = 1$  and  $s = \infty$

## II.C. QMC and Krylov Linear Solvers

The linear and nonlinear solvers come from the Julia package [SIAMFANLEQ.jl](#) [3]. The documentation for these codes is in the [Juila notebooks](#) [4] and the book [5] that accompany the package.

For each example, we use two Krylov methods [6], GMRES [7] and Bi-CGSTAB [8].

### II.C.1. *Garcia-Siewert*

We solve the QMC linear problem with  $N=2048$  and  $N_x=100$ . Figures 1 and 2 show that the Krylov iterations take fewer than half of the number of transport sweeps that Picard iteration required.

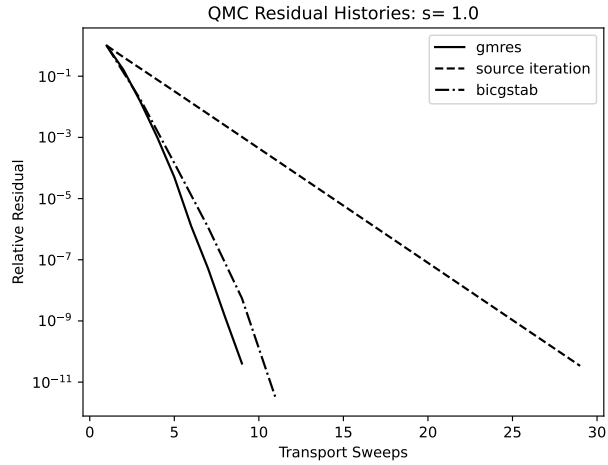


Fig. 1.  $s = 1$

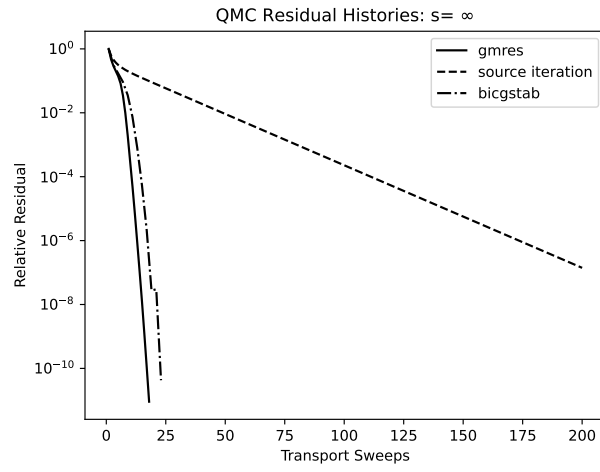


Fig. 2.  $s = \infty$

## II.D. Validation and calibration study

We conclude this section with a validation study. We compare the QMC results with the results from [1]. The results in [1] are exit distributions and are accurate to six figures. We have duplicated those results with an  $Sn$  computation on a fine angular and spatial mesh.

**Sam, Ryan, should we use more or different values of  $N$  and  $Nx$ ?**

For  $N = 2048$  and  $Nx = 100$  we obtain the cell-average fluxes from the QMC approximation. We then use a single  $Sn$  transport sweep to recover the exit distributions from the QMC cell-average fluxes. We report the results and the corresponding results from [1] in Tables I and II.

The exit distributions, as is clear from Table I can vary by five orders of magnitude. Even so, the results from QMC agree with the benchmarks to roughly two figures.

TABLE I  
Exit Distributions:  $s = 1$

$\mu$	Garcia/Siewert		QMC	
	$\psi(0, -\mu)$	$\psi(\tau, \mu)$	$\psi(0, -\mu)$	$\psi(\tau, \mu)$
0.05	5.89664e-01	6.07488e-06	6.07035e-01	5.91908e-06
0.10	5.31120e-01	6.92516e-06	5.47466e-01	6.74075e-06
0.20	4.43280e-01	9.64232e-06	4.57064e-01	9.35453e-06
0.30	3.80306e-01	1.62339e-05	3.92223e-01	1.56108e-05
0.40	3.32964e-01	4.38580e-05	3.43481e-01	4.13721e-05
0.50	2.96090e-01	1.69372e-04	3.05510e-01	1.58622e-04
0.60	2.66563e-01	5.73465e-04	2.75098e-01	5.39514e-04
0.70	2.42390e-01	1.51282e-03	2.50192e-01	1.43257e-03
0.80	2.22235e-01	3.24369e-03	2.29422e-01	3.08975e-03
0.90	2.05174e-01	5.96036e-03	2.11837e-01	5.70555e-03
1.00	1.90546e-01	9.77123e-03	1.96756e-01	9.39189e-03

In Tables III and IV we look at the relative errors in the QMC exit distributions as compared to a highly accurate SN result. We compensate for the widely varying scales by tabulating, for each value of  $N$  and  $Nx$

$$R = \max(R^0, R^\tau)$$

where

$$R^0 = \max_{\mu} \frac{|\psi^{SN}(0, -\mu) - \psi^{QMC}(0, -\mu)|}{\psi^{SN}(0, -\mu)}$$

and

$$R^\tau = \max_{\mu} \frac{|\psi^{SN}(\tau, \mu) - \psi^{QMC}(\tau, \mu)|}{\psi^{SN}(\tau, \mu)}.$$

TABLE II  
Exit Distributions:  $s = \infty$

$\mu$	Garcia/Siewert		QMC	
	$\psi(0, -\mu)$	$\psi(\tau, \mu)$	$\psi(0, -\mu)$	$\psi(\tau, \mu)$
0.05	8.97798e-01	1.02202e-01	9.06050e-01	1.03680e-01
0.10	8.87836e-01	1.12164e-01	8.95849e-01	1.13695e-01
0.20	8.69581e-01	1.30419e-01	8.76487e-01	1.31907e-01
0.30	8.52299e-01	1.47701e-01	8.58937e-01	1.49245e-01
0.40	8.35503e-01	1.64497e-01	8.42195e-01	1.66128e-01
0.50	8.18996e-01	1.81004e-01	8.25870e-01	1.82734e-01
0.60	8.02676e-01	1.97324e-01	8.09780e-01	1.99151e-01
0.70	7.86493e-01	2.13507e-01	7.93834e-01	2.15421e-01
0.80	7.70429e-01	2.29571e-01	7.77997e-01	2.31558e-01
0.90	7.54496e-01	2.45504e-01	7.62269e-01	2.47547e-01
1.00	7.38721e-01	2.61279e-01	7.46673e-01	2.63362e-01

Ryan, for large  $N_x$  I see convergence as  $N$  increases. Is it clearly  $1/N$ ? Am I missing something? Am I tabulating the wrong thing?

TABLE III  
Exit Distributions Errors:  $s = 1.0$

$N_x \setminus N$	1024	2048	4096	8192	16384
50	1.31716e-01	1.34260e-01	1.35123e-01	1.35328e-01	1.35242e-01
100	6.09631e-02	6.35764e-02	6.46191e-02	6.48898e-02	6.48536e-02
200	3.77223e-02	3.12496e-02	3.12005e-02	3.17337e-02	3.16710e-02
400	2.63214e-02	1.45106e-02	1.52355e-02	1.56636e-02	1.56854e-02
800	2.39486e-02	9.94925e-03	7.24627e-03	8.86212e-03	7.84063e-03
1600	4.16277e-02	9.95048e-03	5.11618e-03	8.02709e-03	4.44021e-03
3200	4.60905e-02	1.07345e-02	4.45922e-03	7.49522e-03	3.76179e-03

#### II.D.1. Multigroup Problems

These are preliminary results with  $N_x = 40$  and  $N = 2^{10}$ . We may want to make these larger and/or make tables like Table III and Table III.



TABLE IV  
Exit Distributions Errors:  $s = \infty$

$N_x \setminus N$	1024	2048	4096	8192	16384
50	1.31716e-01	1.34260e-01	1.35123e-01	1.35328e-01	1.35242e-01
100	6.09631e-02	6.35764e-02	6.46191e-02	6.48898e-02	6.48536e-02
200	3.77223e-02	3.12496e-02	3.12005e-02	3.17337e-02	3.16710e-02
400	2.63214e-02	1.45106e-02	1.52355e-02	1.56636e-02	1.56854e-02
800	2.39486e-02	9.94925e-03	7.24627e-03	8.86212e-03	7.84063e-03
1600	4.16277e-02	9.95048e-03	5.11618e-03	8.02709e-03	4.44021e-03
3200	4.60905e-02	1.07345e-02	4.45922e-03	7.49522e-03	3.76179e-03

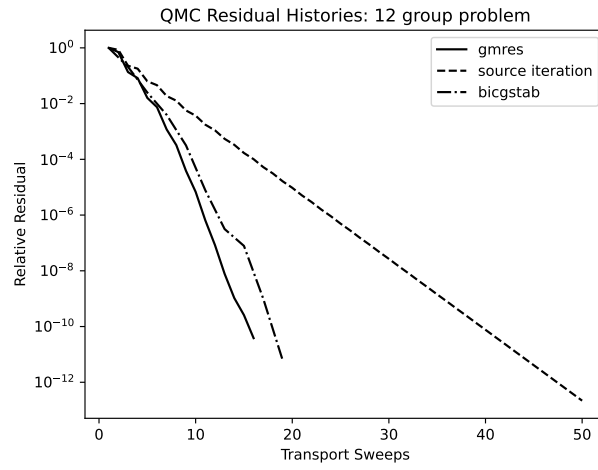


Fig. 3

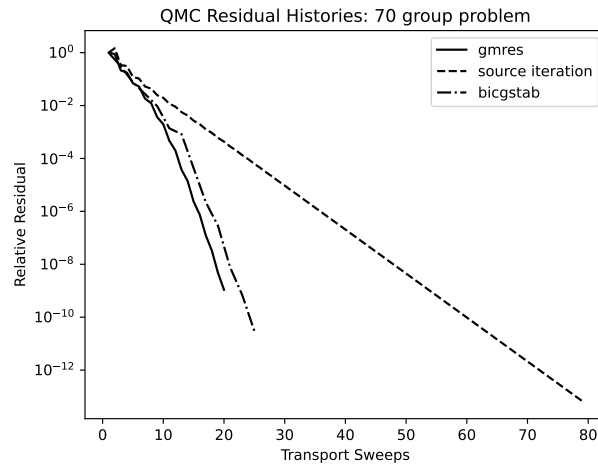


Fig. 4

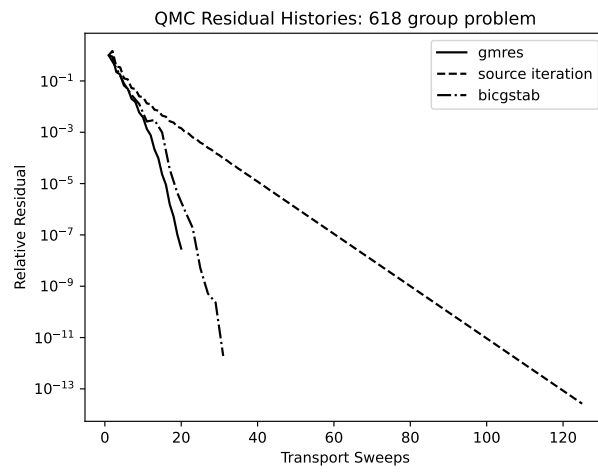


Fig. 5

### III. CONCLUSION

## **ACKNOWLEDGMENTS**

The research of CTK was supported by Department of Energy grant DE-NA003967, and National Science Foundation Grants DMS-1745654, and DMS-1906446.

## REFERENCES

- [1] R. GARCIA and C. SIEWERT, “Radiative transfer in finite inhomogeneous plane-parallel atmospheres,” *J. Quant. Spectrosc. Radiat. Transfer*, **27**, 141 (1982).
- [2] J. WILLERT, C. T. KELLEY, D. A. KNOLL, and H. K. PARK, “Hybrid Deterministic/Monte Carlo Neutronics,” *SIAM J. Sci. Comp.*, **35**, S62 (2013).
- [3] C. T. KELLEY, “SIAMFANLEquations.jl,” <https://github.com/ctkelley/SIAMFANLEquations.jl> (2020); 10.5281/zenodo.4284807., URL <https://github.com/ctkelley/SIAMFANLEquations.jl>, julia Package.
- [4] C. T. KELLEY, “Notebook for Solving Nonlinear Equations with Iterative Methods: Solvers and Examples in Julia,” <https://github.com/ctkelley/NotebookSIAMFANL> (2020); 10.5281/zenodo.4284687., URL <https://github.com/ctkelley/NotebookSIAMFANL>, iJulia Notebook.
- [5] C. T. KELLEY, “Solving Nonlinear Equations with Iterative Methods: Solvers and Examples in Julia,” (2020) Unpublished book ms, under contract with SIAM.
- [6] C. T. KELLEY, *Iterative Methods for Linear and Nonlinear Equations*, no. 16 in Frontiers in Applied Mathematics, SIAM, Philadelphia (1995).
- [7] Y. SAAD and M. SCHULTZ, “GMRES a generalized minimal residual algorithm for solving nonsymmetric linear systems,” *SIAM J. Sci. Stat. Comp.*, **7**, 856 (1986).
- [8] H. A. VAN DER VORST, “Bi-CGSTAB: A fast and smoothly converging variant to Bi-CG for the solution of nonsymmetric systems,” *SIAM J. Sci. Statist. Comput.*, **13**, 631 (1992).